

Mechanism of resistance degradation of lead magnesium Niobate-based ferroelectrics induced by hydrogen reduction during electroplating

JIANG LI CAO*, LONG TU LI, YONG LI WANG,
JIAN QIANG ZHAO, ZHI LUN GUI

State Key Laboratory of New Ceramic and Fine Processing, Department of Materials Science and Engineering, Tsinghua University, Beijing 100084, People's Republic of China
E-mail: perov@sina.com

Resistive leakage of lead magnesium niobate (PMN) based relaxor ferroelectrics after nickel electroplating was investigated through X-ray photoelectronic spectroscopy (XPS) analysis and annealing experiments in oxygen and argon. It was found that the resistivity of the ceramics declined nonlinearly with the electroplating time. XPS analysis suggested that the reduction of Nb^{5+} to Nb^{4+} by hydrogen during electroplating played an important role in the degradation. It was also noted that the degraded specimen can recover its properties completely after oxygen annealing at 600°C for 1 hour through the oxidation of Nb^{4+} to Nb^{5+} . In contrast, almost no oxidization of Nb^{4+} and improvement of the degradation were observed for the degraded specimen after argon annealing. Therefore, it was concluded that the resistance degradation of the PMN-based relaxor ferroelectrics during electroplating must be ascribed to the oxygen loss and the reduction of Nb^{5+} to Nb^{4+} .

© 2002 Kluwer Academic Publishers

1. Introduction

Multilayer ceramic capacitors (MLCC) are in increasing demand because of the rapid development of surface mounting technology and the trend of miniaturization of electronic circuitry. PMN, a kind of complex perovskite oxide has been intensively studied due to its wonderful properties, such as high dielectric constant, diffuse phase transition and relatively low sintering temperature (1–4). As one of the most important material systems in MLCC industry, PMN-based relaxor ferroelectrics has been widely used.

In MLCC fabrication, three-layer-electrode technique is generally adopted, i.e., Ag ground/ $2\text{--}4\ \mu\text{m}$ Ni coating/ $4\text{--}10\ \mu\text{m}$ Sn or Sn-Pb alloy coating. Firstly, Ag ground is fired on the terminations of MLCC. Then Ni is electroplated on the Ag ground as a barrier against Ag diffusion. Finally, Sn or Sn-Pb alloy is electroplated to improve the solderability. Terminations with this structure can well meet the solderability specification without damaging the functional properties of MLCC. However, it was found that PMN-based MLCC were sensitive to the electroplating parameters [5–7]. The main electrical properties of electroplated PMN-based MLCC sometimes deteriorated partially or even completely after electroplating. Among them, resistance degradation was a common one. This indicated that the electroplating may have a negative influence on

the PMN-based MLCC. Moreover, it was noted that some electroplated PMN-based MLCC could not pass the temperature-humidity-bias test (THB) whereas the uncoated one can easily meet this specification.

Much effort has been dedicated to the improvement of PMN-based MLCC against electroplating and the understanding of the failure mechanism [6–8]. In previous studies, active atomic hydrogen generated during electroplating has been firstly emphasized [9] and the reduction of metal elements in the PMN-based relaxor ferroelectrics was proposed [10]. However, as to the role of hydrogen in the reduction, there are still two hypotheses that explain the resistance degradation. One hypothesis suggests that the metal elements may be reduced to lower valence states, which is accompanied by the generation of oxygen vacancies. The other one believes that active hydrogen atoms can be incorporated into the perovskite lattice, thereby lead to the functional degradation of the ceramics. Both of the hypotheses can theoretically explain the resistance degradation. The goal of this study was to find the intrinsic reason for the degradation of PMN-based relaxor ferroelectrics during electroplating. The results were discussed and the mechanism of hydrogen action was clarified on the basis of XPS analyses in connection with the annealing experiments in air and argon respectively at elevated temperature.

*Author to whom all correspondence should be addressed.

TABLE I Nickel electroplating process parameters

Nickel sulfamate ($\text{g} \cdot \text{l}^{-1}$)	60
NiCl_2 ($\text{g} \cdot \text{l}^{-1}$)	15
Boric acid ($\text{g} \cdot \text{l}^{-1}$)	40
pH	3.8
Temperature ($^{\circ}\text{C}$)	55
Cathodic current density ($\text{A} \cdot \text{dm}^{-2}$)	1.0

2. Experimental details

The specimens studied were $0.98\text{Pb}(\text{Mg}_{1/3}\text{Nb}_{2/3})\text{O}_3-0.01\text{Pb}(\text{Zn}_{1/3}\text{Nb}_{2/3})\text{O}_3-0.01\text{PbTiO}_3$ relaxor ferroelectrics (abbreviated for PMZNT). This composition can meet the EIA Y5V specification and has been commercialized [11]. The ceramic powders were prepared through a conventional two-stage calcination method with reagent grade oxides applied. Firstly MgNb_2O_6 and ZnNb_2O_6 were prepared. Then PbO and TiO_2 were added to the two previously calcined precursors. After being calcined, ball-milled and dried, the powders were dry-pressed into pellets with a diameter of 1 cm. Sintering was carried out at 970°C for 4 hours followed by cooling down in the furnace with the pellets buried under the ceramic powders. Finally, Ag terminations were calcined on the specimens.

Before being electroplated, the specimens were subjected to chemical cleaning and activation. Then the specimens were electroplated in a nickel-sulfamate based solution with slight mechanical agitation. Commercial additives were added to keep the coating smooth and minimize the internal stress in the coating. Composition of nickel electroplating solution and processing parameters are listed in Table I.

The resistivity was measured by applying 10 V DC to the specimens for 1 min at room temperature, using a HP4140B pA meter. The annealing experiments on plated specimens were conducted respectively in air and argon (1.5 atm , $P_{\text{O}_2} \leq 15 \text{ Pa}$) at 600°C for 1 hour, with a constant heating rate of 300°C per hour applied.

XPS analysis was carried out at room temperature on a PHI 5300 ESCA/610 SAM of Perkin Elmer with a spherical capacitance analyzer (SCA). Al K_{α} X-ray was adopted as the excitation source operating at 250 W. Vacuum pressure of the instrument chamber was $1 \times 10^{-7} \text{ Pa}$ as read on the panel. The size of detected area was $1 \times 3 \text{ mm}^2$. Measured spectra were decomposed into Gaussian components by a least-squares fitting method. Binding energy was calibrated with reference to C1s peak (285.0 eV).

3. Results

3.1. Resistivity characteristics of the ceramics after nickel electroplating

Resistivity changes of the PMZNT ceramics after nickel electroplating were measured as a function of the electroplating time. As shown in Fig. 1, it can be seen that the resistivity decreased nonlinearly after the electroplating. After 3 hours of plating, the resistivity decreased by about two orders of magnitude. It was also noted that the ceramics became darker as the electroplating continued, while the blank specimens were brown.

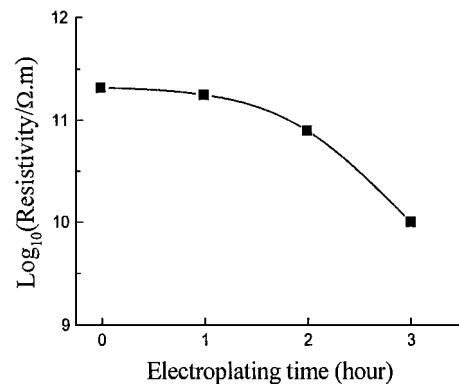


Figure 1 Resistivity changes of the PMZNT ceramics after nickel electroplating.

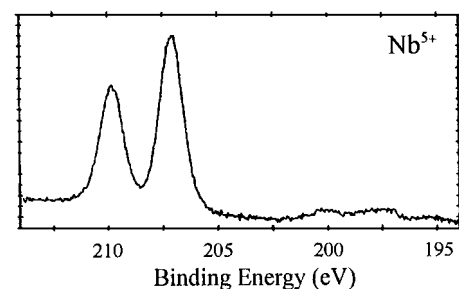


Figure 2 Narrow spectrum of Nb3d of the PMN-based ferroelectrics.

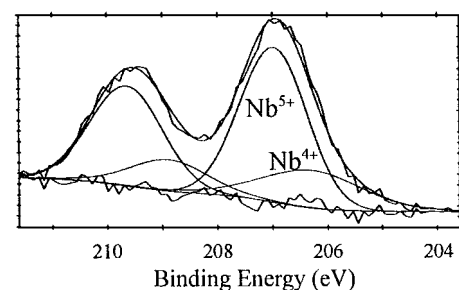


Figure 3 Narrow scan of Nb3d spectrum of a 3 hour-plated specimen.

3.2. XPS analyses

XPS technique was adopted to study the possible chemical reactions involved in the resistance degradation. Valence stages of metal elements in the PMZNT ceramics before and after the electroplating were examined. Fig. 2 plots the narrow spectrum of Nb in a blank specimen. The binding energy of Nb 3d_{5/2} was 207.1 eV and the splitting about 2.8 eV. Judging from these values, the authors believed that Nb in the PMZNT was in +5 state [12, 13]. Then the Nb spectrum on a 3 hour-plated specimen was measured as shown in Fig. 3. After curve fitting, it can be seen that a new component appeared at the lower energy side. The deconvoluted curve represented the raw spectrum while the smooth one the numerically fitted component. Nb3d_{5/2} binding energy of the new component was 206.1 eV that was in accordance with Nb⁴⁺ in NbO₂ [12, 13]. The ratio of the new component to Nb⁵⁺ was about 1 : 3, which indicates that a part of Nb⁵⁺ in the PMN-based ceramics has been reduced to Nb⁴⁺. In the present experiment, no valence change was detected for other metal elements in PMZNT ceramics.

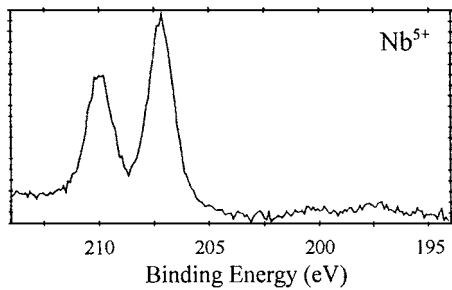


Figure 4 Spectrum of Nb3d of the degraded specimen after annealing in air at 600°C for 1 hour.

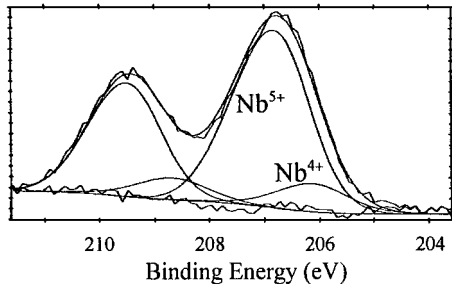


Figure 5 Nb3d spectrum of the degraded specimen after annealing in argon at 600°C for 1 hour.

3.3. Annealing experiments on the plated specimens

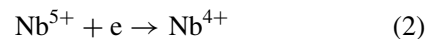
To verify the effect of Nb^{5+} reduction to Nb^{4+} on the resistivity changes of PMZNT, annealing experiments on the 3 hour-plated ceramic specimens at 600°C were carried out in air and argon respectively. After air annealing, the resistivity of the specimens recovered completely and the color turned brown, whereas nearly no change was observed for the argon-annealed specimens. In the same way, XPS analysis was undertaken to examine the valence states of Nb in the annealed ceramics. Fig. 4 shows the narrow scan of Nb spectrum of the air-annealed ceramics. It can be seen that there was only one component in the Nb spectrum and the binding energy of Nb3d5/2 was 207.1 eV. By comparison to Fig. 3, it indicated that Nb^{4+} was oxidized to Nb^{5+} totally. Fig. 5 presents the Nb spectrum of the degraded ceramics after argon annealing. Different from Fig. 4, there was still one component at the lower binding energy side. After resolution, it was found that the binding energy of the component was 206.1 eV. This suggested that the Nb^{4+} in the plated ceramics was slightly oxidized and Nb^{4+} concentration only changed little, which was evidently different from the air annealing results.

4. Discussions

In this paper, effect of nickel electroplating on the resistance characteristics of PMN-based relaxor ferroelectrics was studied. XPS analysis on the plated specimen showed that a part of Nb^{5+} had been reduced to Nb^{4+} during nickel electroplating. The air annealing at elevated temperature can completely restore the plated specimens through which all of the Nb^{4+} in the ceramics was re-oxidized to Nb^{5+} . In contrast, no resistance recovery was detected for the plated specimens after argon annealing. Correspondingly, there were still much Nb^{4+} in the ceramics. All these results suggested that

the reduction of metal elements in the PMN-based ceramics during electroplating should be responsible for the resistance degradation.

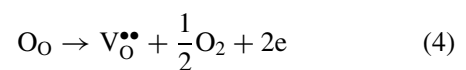
As well known, hydrogen can be generated during electroplating as the byproduct. At initial stage, hydrogen can be absorbed on the cathode in the form of hydrogen atoms. These atoms may then diffuse along the cathode surface and react with the substrate. In the present study, the PMN-based ceramics suffered the hydrogen reduction evidently and a part of Nb^{5+} was reduced to Nb^{4+} , as described in Equations 1 and 2. It is easy to prove the feasibility of the chemical reaction according to thermodynamics.



From the viewpoint of defect chemistry, the electroplating treatment can be considered to supply a reducing atmosphere through the side reaction of hydrogen generation. During the reaction, hydrogen are ionized, releasing one electron. As to how hydrogen atoms act during the reduction, however, there are two different hypotheses. The first one believes that hydrogen can penetrate into the perovskite lattice and be incorporated into the oxygen octahedral as an interstitial atom, giving one electron to metal ions (Equation 3). The ionization of hydrogen atoms will lower the resistivity of the ceramics. In previous works, resistance degradation of $\text{Pb}(\text{Zr}, \text{Ti})\text{O}_3$ with perovskite structure induced by hydrogen annealing has been studied, which was in accordance with this mechanism [14].



Different from the hypothesis above, the other one supports that oxygen ions may be lost from the perovskite lattice while oxygen vacancies and electrons are produced with the reduction of metal elements (Equation 4).



As new charge carriers in the dielectric ceramics, oxygen vacancies and electrons increase as the electroplating continues, lowering the resistivity of the ceramics.

Seeing this, it is difficult to identify these two hypotheses just according to the XPS analysis on the degraded specimen (Figs 2 and 3). Hence, annealing experiments in air and argon were conducted respectively. As can be seen in Figs 3 and 4, all of Nb^{4+} in the degraded specimen was oxidized to Nb^{5+} through air annealing at high temperature whereas almost no, if any, only little Nb^{4+} was oxidized through the argon annealing. Moreover, the resistivity measurement clarified the resistance characteristics of the annealed samples and reinforced the key role of Nb^{5+} reduction in the degradation.

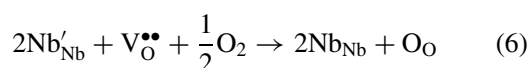
In view of hydrogen penetration hypothesis, it can be inferred that during air annealing at high temperature, hydrogen may obtain one electron and then diffuse out of the oxygen octahedral owing to the high temperature and low hydrogen partial pressure (Equation 5). Meanwhile, Nb^{4+} should be oxidized to Nb^{5+} , thereby the

resistivity of the specimen is restored. The reaction is just the reverse reaction of Equation 3.



Or stated differently the resistivity recovery and Nb^{4+} oxidation to Nb^{5+} are ascribed to the reduction of hydrogen ions and the following diffusion while the atmosphere has no effect on this change. However, this hypothesis is obviously contradicted to the argon annealing experiment, in which still most of Nb^{4+} existed in the ceramics and no resistivity recovery was observed. Considering oxygen impurity in argon and the furnace, the small change of Nb^{4+} concentration may be attributed to the oxygen in the atmosphere. That is to say, argon annealing has no, if any, only little effect on the oxidization of Nb^{4+} to Nb^{5+} and the oxygen ambient is necessary to restore the degraded ceramics. Therefore, the hydrogen penetration hypothesis neglects the participation of oxygen vacancies during the degradation and recovery and is considered to be uncertain.

With regard to the second hypothesis of oxygen vacancy generation, it can well explain the results presented in this paper. Oxygen vacancies are created in the perovskite lattice with the reduction of Nb^{5+} to Nb^{4+} caused by the reducing atmosphere of hydrogen atoms. The involvement of oxygen ionic and electronic conduction answers for the resistivity deterioration of the ceramics after electroplating. Among them, oxygen vacancy conduction may be small owing to their poor mobility near room temperature. During air annealing, oxygen in the atmosphere diffuses into the perovskite lattice and Nb^{4+} are oxidized to Nb^{5+} , through which charge carriers are minimized according to equation 6.



Correspondingly, the resistivity of the plated ceramics is restored. That is to say, the oxidation of Nb^{4+} to Nb^{5+} results from the oxygen ambient, but not the hydrogen diffusion-out. Because there was just little oxygen in the argon atmosphere, Nb^{4+} can not be oxidized through the argon annealing and, therefore, oxygen vacancy concentration remained almost unchanged. As a result, no resistance recovery was detected for the degraded specimens after argon annealing.

5. Conclusions

1. The resistivity degradation of PMN-based ceramics during electroplating was attributed to the hydrogen reduction.

2. XPS analysis indicated that Nb^{5+} in the ceramics can be reduced to Nb^{4+} during nickel electroplating.

3. As a result of Nb^{4+} reduction, oxygen vacancies were created and ionic and electronic conduction were involved, which led to the resistance degradation of the PMN-base relaxor ferroelectrics.

Acknowledgements

The authors are indebted to the financial support from the National Natural Science Foundation of P. R. China (Grant: 59995523). Dr. Ning Xin Zhang is appreciated for his useful discussions.

References

1. S. L. SWARTZ and T. R. SHROUT, *Mater. Res. Bull.* **17** (1982) 1245.
2. S. L. SWARTZ, T. R. SHROUT, W. A. SCHULZE and L. E. CROSS, *J. Amer. Ceram. Soc.* **67** (1984) 311.
3. D. J. VOSS, S. L. SWARTZ and T. R. SHROUT, *Ferroelectrics* **50** (1983) 203.
4. Z. KIGHELMAN, D. DAMJANOVIC, A. SEIFERT, L. SAGALOWICZ and N. SETTER, *Appl. Phys. Lett.* **73** (1998) 2281.
5. A. MOORE, *Electronic Production* **18** (1989) 25.
6. D. A. BEHM, C. J. FELTZ, R. HAYNES and S. C. PINAULT, *J. Amer. Ceram. Soc.* **72** (1989) 2279.
7. F. R. ANDERSON, R. HAYNES and S. C. PINAULT, *IEEE Transaction on Components, Hybrids, and Manufacturing Technology* **12** (1989) 609.
8. H. C. LING and A. M. JACKSON, *IEEE Transactions on Component, Hybrids, and Manufacturing Technology* **12** (1989) 130.
9. W. P. CHEN, L. T. LI, Y. WANG and Z. L. GUI, *J. Mater. Res.* **13** (1998) 1110.
10. J. L. CAO, L. T. LI and Z. L. GUI, *J. Mater. Chem.* **11** (2001) 1198.
11. Z. L. GUI, Y. WANG and L. T. LI, Proc. the Tenth IEEE Intern. Symp. on Appl. of Ferro., August 18, 1996, p. 409.
12. J. F. MOULDER, W. F. STICKLE, P. E. SOBOLE and K. D. BOMBEN, "Handbook of X-ray Photoelectron Spectroscopy" (Perkin-Elmer Corporation, USA, October, 1992).
13. M. Z. ATASHBAR, H. T. SUN, B. GONG, W. WLODARSKI and R. LAMB, *Thin Solid Film* **326** (1998) 238.
14. S. AGGARWAL, S. R. PERUSSE, C. J. KERR, R. RAMESH, D. B. ROMERO, J. T. EVANS, JR., L. BOYER and G. VELASQUEZ, *Appl. Phys. Lett.* **76** (2000) 918.

Received 29 June 2001

and accepted 17 April 2002